Non-Isothermal Channel Flow of Non-Newtonian Fluids with Viscous Heating

Approximate analytical solutions of the local temperature variations, due to viscous heating, in channel flows of non-Newtonian fluids with small Nahme-Griffith numbers were obtained by the WKB-J method. The results are general and easy to use so that extensive numerical computations are not required. Comparisons between the approximate analytical solution and complete numerical solution showed that the relative differences were very small.

S. M. DINH and R. C. ARMSTRONG

Department of Chemical Engineering
and
MIT-Industry Polymer Processing Program
Massachusetts Institute of Technology
Cambridge, MA 02139

SCOPE

The large usage of polymeric materials has raised numerous fundamental questions that need to be understood in order to maximize the efficiency of processing these materials. Proper temperature control of the polymer is a major factor in determining the quality of the final product. For example in the processing of thermoplastics, the solid polymer is melted prior to forming. This phase change is usually accomplished by means of external heaters and by viscous heat generated during flow. It is important to be able to calculate the degree of viscous heating so that the amount of heat required from external sources can be estimated. In addition, it is necessary to be sure that the polymer is not overheated because this might result in degradation of the material. For this reason, we also need to compute local temperature values to be sure that these are not significantly different from the bulk temperature. For thermosetting polymers it is also important to be able to calculate the local temperature rise due to viscous heating so as to be able to prevent premature reactions in the molding compound.

Previous workers in this area have attempted to solve the Graetz problem for specific fluids with specific boundary conditions, for example, for a Newtonain fluid flowing in a tube with isothermal walls. These earlier analytical solutions for the local temperature profile did not agree closely with corresponding numerical solutions, because the analytical solution was not valid uniformly over the cross-section of the channel. Hence several solutions had to be matched, but the matching regions were uncertain.

The objective of this paper is to provide simple, analytical, uniformly valid solutions for evaluating the local temperature rise due to viscous heating in confined channel flows of non-Newtonian fluids. Our solutions are good for any viscosity-shear rate relationship, but they are restricted to fluids with small Nahme-Griffith members, i.e., fluids whose viscosities are independent of temperature.

CONCLUSIONS AND SIGNIFICANCE

In this paper we have developed a general analytical solution for the local temperature change due to viscous heating for non-Newtonian fluids undergoing channel flows with arbitrary wall heat transfer coefficient. In previous studies the temperature has been calculated only by numerical methods. We have considered a special class of non-Newtonian fluids that is characterized by a small Nahme-Griffith number (fluids with rheological properties that are insensitive to temperature); however, the results are good for any viscosity-shear rate relationship and consequently can describe behavior of a wide variety of non-Newtonian fluids over wide ranges of shear rate.

The temperature field is obtained by combination of the WKB-J and Langer's methods. The results for the temperature profiles are exceedingly accurate, with our analytical solutions being indistinguishable from numerical calculations. Moreover, the agreement between our eigenvalues and numerical results were worst for the lowest eigenvalue; in all the cases we considered the two calculations of this eigenvalue were within 10% of one another, and by the second eigenvalue the two were within 1%.

The results obtained here should be useful not only for low Nahme-Griffith number problems but also when viscosity depends on temperature. In this latter case our solutions could be incorporated into a numerical scheme such as that of Winter (1977) to eliminate iterations required to compute temperature from the energy equation once the viscosity is given as a function of position.

INTRODUCTION

In the processing of polymeric materials by, for example, extrusion or injection molding, molten polymer is typically forced through confined channels at relatively high speeds so as to minimize the cycle time in fabricating a part. As a result, the polymer encounters a high rate of deformation. In addition, most polymers have high viscosities and low thermal conductivities, which in combination with large process shear rates can lead to significant increases in temperature from viscous heating. Moreover, these temperature rises can be highly non-uniform with local temperature rises in great excess over the mean temperature rise (Pearson, 1978).

The consequences of such temperature rises can be beneficial or detrimental to the process. One advantage is that an increase in temperature lowers the viscosity, and thereby makes a given flow rate possible with lower pressure drops. However, the decrease in viscosity with increasing temperature exaggerates the concentration of shearing near the wall. This tends to localize viscous heating and can, by virtue of the low thermal conductivity, lead to unexpectedly large local temperature rises. Severe rises in temperature can lead to degradation in thermoplastics, or trigger prematue reactions in thermosets. Hence it is important to be able to estimate the local temperature change in the system due to viscous heating so that

0001-1541-82-5508-0294-$2.00

the maximum processing temperature can be properly controlled.

There have been several previous studies of the viscous heating problem. For constant physical properties and large Peclet number, the problem is usually solved by separation of variables. The eigenvalue problem which arises in this method (often referred to as the Graetz problem) has been analyzed both analytically and numerically. Ziegenhagen (1965) used the WKB-J method to calculate the eigenvaluues for a power-law fluid in tubes with insulated or isothermal walls. However, he was unable to evaluate accurately the temperature profiles because of a lack of a global solution for the eigenfunctions. Sellars et al. (1956) used the same method for Newtonian fluids, but in tubes with arbitrary wall temperature and heat-flux variations. However, as in Ziegenhagen's solution, they were unable to evaluate precisely the temperature field because they lacked a uniformally valid approximation to the eigenfunctions. In both of these studies, different approximations to the eigenfunctions are given in different regions of the channel, but it is not known precisely where the boundaries between these approximations lie. More recently Ybarra and Eckert (1980) have solved the eigenvalue problem by using a finite difference method. In this way they avoid the difficulty in matching various approximate solutions and are able to compute temperature profiles. In their paper they report results for a power-law fluid, and we compare these with our results in Section II.

If the physical properties of the fluid are temperature dependent, then a numerical approach is almost inevitable. Winter (1977) used a finite difference method to examine heat transfer problems with viscous heating in shearing flows. In his solution the viscosity of the power law fluid depends exponentially on temperature, and the boundary conditions at the wall were represented by an arbitrary, constant heat transfer coefficient. Gerrard et al. (1965, 1966) also utilized a finite difference procedure, but with non-uniform grid size, to estimate the temperature rise in tube flow for a Newtonian fluid where the walls are isothermal or insulated. However, they included a term for radial convective heat transfer in the energy equation; they also allowed the viscosity to depend on pressure and temperature. In addition Gerrard et al. experimentally measured the local pressure and temperature variations, and these were within 5% of the predicted values.

For fluids with high thermal conductivity or when the Peclet number is small then axial conduction may no longer be negligible. This class of problem has been recently explored by Papoutsakis et al. (1980) and Acrivos (1980).

The objective of this work is to provide simple analytical solutions for estimating the local temperature rise from viscous heating in slit flow and tube flow of non-Newtonian fluids. In our calculations we assume heat transfer from the wall can be described by a constant, arbitrary heat transfer coefficient. In order to obtain relatively simple closed-form solutions we also assume that the physical properties of the fluid do not depend on temperature. This assumption is most serious for the viscosity, for which it corresponds to small values of the Nahme-Griffith number (Pearson, 1978; Winter, 1977). This is not necessarily overly restrictive as we discuss in the final section.

SLIT PROBLEM

Problem Description and Assumptions

Figure 1 shows a cross section of the slit flow problem that we want to consider here. The half-thickness of the slit is much smaller than the width (into the page), and the fluid flows in the $+z$-direction under a constant pressure gradient dp/dz. Prior to the plane $z = 0$, the fluid is at uniform temperature T_o; for $z > 0$ viscous heating acts to produce local temperature variations in both x and z. The walls of the slit are at T_o for $z < 0$, whereas for $z > 0$ the heat flux to the wall q_x is given by a heat transfer coefficient h:

$$q_x(z) = h[T(B,z) - T_o] \tag{1}$$

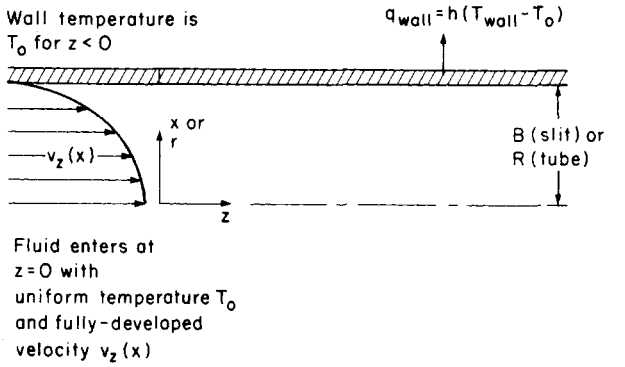

Figure 1. Slit and tube flow geometries studied for the viscous heating problem.

In our solution we consider arbitrary values of h as well as the limiting cases of infinite h (isothermal wall) and h equal to zero (insulated wall).

The fluid flowing in the slit is taken to be a purely viscous non-Newtonian fluid whose viscosity η depends on the shear rate $\dot{\gamma}(= |dv_z/dx|)$. In addition we make the following assumptions:

1. The physical properties of the fluid, in particular the viscosity, are independent of temperature.
2. The velocity profile is fully developed prior to $z = 0$.
3. Axial conduction is small compared to axial convection.

Governing Equations

For the assumptions given above, the equations of motion and energy for this problem are:

$$0 = -\frac{dp}{dz} + \frac{d}{dx}\eta\frac{dv_z}{dx} \tag{2}$$

$$\rho\hat{C}_p v_z \frac{\partial T}{\partial z} = k\frac{\partial^2 T}{\partial x^2} + \eta(\dot{\gamma})\dot{\gamma}^2 \tag{3}$$

Because we assume the velocity profile is fully developed and η is independent of temperature, Eq. 2 can be solved separately from Eq. 3 to give the velocity field for all z. As an example, the power-law model for viscosity

$$\eta = m\dot{\gamma}^{n-1} \tag{4}$$

in which m is the consistency index and $(n - 1)$ is the power law slope, leads to

$$v_z = \left(-\frac{1}{m}\frac{dp}{dz}\right)^s \frac{B^{s+1}}{s+1}\left[1 - \left(\frac{x}{B}\right)^{s+1}\right]$$
$$= V_{max}[1 - \xi^{s+1}] \tag{5}$$

where $s = 1/n$. In the second line of Eq. 5 we have introduced the dimensionless coordinate $\xi = x/B$. It is convenient in what follows to define a dimensionless velocity ϕ by

$$\phi(\xi) = v_z/V_{max} \tag{6}$$

With this choice of dimensionless velocity and position, the shear rate is written

$$\dot{\gamma} \equiv |dv_z/dx| = \frac{V_{max}}{B}\left|\frac{d\phi}{d\xi}\right| \tag{7}$$

This suggests that for the power-law model a convenient choice of dimensionless viscosity η_r is

$$\eta_r \equiv \frac{\eta}{m\left(\frac{V_{max}}{B}\right)^{n-1}} = \left|\frac{d\phi}{d\xi}\right|^{n-1} \tag{8}$$

For the slit flow velocity field in Eq. 4, the reduced power-law viscosity varies with position according to

$$\eta_r = (s+1)^{1/s-1}\xi^{1-s} \tag{9}$$

In general, if the viscosity model of interest contains the zero-shear-rate viscosity η_o then η_r is defined by η/η_o.

It remains to solve the energy equation. Equation 3 can be put in the dimensionless form

$$\phi \frac{\partial \theta}{\partial \zeta} = \frac{\partial^2 \theta}{\partial \xi^2} + \eta_r \left(\frac{d\phi}{d\xi}\right)^2 \tag{10}$$

in which $\theta = (T - T_o)k/V^2_{max}\eta_o$ and $\zeta = kz/\rho \hat{C}_p V_{max} B^2$. For the power-law fluid, the η_o appearing in the definition for θ is taken to be $\eta(V_{max}/B) = m(V_{max}/B)^{n-1}$. The boundary conditions that go with Eq. 10 are

$$\text{at } \zeta = 0, \theta = 0 \tag{11}$$

$$\text{at } \xi = 0, \frac{\partial \theta}{\partial \xi} = 0 \tag{12}$$

$$\text{at } \xi = 1, \begin{cases} \dfrac{\partial \theta}{\partial \xi} = -N\theta & \text{arbitrary wall heat transfer} \quad (13a) \\ \dfrac{\partial \theta}{\partial \xi} = 0 & \text{adiabatic} \quad (13b) \\ \theta = 1 & \text{isothermal wall} \quad (13c) \end{cases}$$

where $N = hB/k$ is a Biot modulus. Obtaining an analytical solution to the above set of equations is the main objective of this paper. In the following discussion, we treat the adiabatic problem separately from the arbitrary heat transfer and isothermal wall problems. The reason for this distinction is that the solutions are physically different in character in these situations. As long as the Biot number N is non-zero (Eqs. 13a and c) then there will exist a fully-developed temperature profile. However when $N = 0$, the fluid has no way to get rid of heat so as to produce a steady balance with viscous heat generation; as a result the shape of the temperature profile becomes fixed but the temperature grows without limit as $\zeta \to \infty$.

Fully-Developed Flow Solution

For a non-zero Biot modulus we postulate a solution of the form

$$\theta(\xi, \zeta) = \theta_1(\xi) - \sum_i c_i X_i(\xi) \exp(-a_i \zeta) \tag{14}$$

where θ_1 is the fully-developed temperature profile and must be the solution to the ordinary differential equation

$$\frac{d^2\theta_1}{d\xi^2} = -\eta \left(\frac{d\phi}{d\xi}\right)^2 \tag{15}$$

with

$$\frac{d}{d\xi}\theta_1(0) = 0 \text{ and } \frac{d}{d\xi}\theta_1(1) = -N\theta_1(1) \tag{16}$$

From these equations the fully-developed temperature profile is found to be

$$\theta_1(\xi) = \frac{1}{N}\int_0^1 \eta_r(\xi')\left(\frac{d\phi}{d\xi'}\right)^2 d\xi' + (1-\xi)\int_0^\xi \eta_r(\xi') \times \left(\frac{d\phi}{d\xi'}\right)^2 d\xi' + \int_\xi^1 (1-\xi')\eta_r(\xi')\left(\frac{d\phi}{d\xi'}\right)^2 d\xi' \tag{17}$$

The developing part of the temperature profile is obtained by the method of separation of variables as indicated in the last term in Eq. 14. The eigenfunctions X_i and eigenvalues a_i are the solutions to

$$\frac{d^2X}{d\xi^2} + a\phi(\xi)X(\xi) = 0 \tag{18}$$

$$\frac{dX}{d\xi}(0) = 0 \tag{19a}$$

$$\frac{dX}{d\xi}(1) = -NX(1) \tag{19b}$$

Once the X_i and a_i are found the expansion coefficients c_i are obtained from the initial conditions by taking advantage of the orthogonality of the eigenfunctions over the interval 0 to 1 with respect to the weight function ϕ:

$$c_i = \frac{\int_0^1 \theta_1(\xi)\phi(\xi)X_i(\xi)d\xi}{\int_0^1 \phi(\xi)X_i^2(\xi)d\xi} \tag{20}$$

For the insulated wall problem we anticipate an additional contribution to the temperature profile that grows continuously with ζ and which reflects the unbalanced heating of the fluid as it flows downstream:

$$\theta(\xi, \zeta) = \theta_1(\xi) + D_o\zeta - \sum_i c_i X_i(\xi)\exp(-a_i\zeta) \tag{21}$$

The ultimate shape of the temperature profile θ_1 is the solution to

$$\phi D_0 = \frac{d^2\theta_1}{d\xi^2} + \eta_r(\xi)\left(\frac{d\phi}{d\xi}\right)^2 \tag{22}$$

$$\frac{d\theta_1}{d\xi}(0) = 0 \tag{23a}$$

$$\frac{d\theta_1}{d\xi}(1) = 0 \tag{23b}$$

Equations 22 and 23 can be integrated easily to give

$$\theta_1(\xi) = \int_0^\xi (\xi - \xi')\left[D_0\phi(\xi') - \eta_r(\xi')\left(\frac{d\phi}{d\xi'}\right)^2\right] d\xi' \tag{24}$$

where

$$D_0 = \frac{\int_0^1 \eta_r(\xi')\left(\frac{d\phi}{d\xi'}\right)^2 d\xi'}{\int_0^1 \phi(\xi')d\xi'} \tag{25}$$

The developing part of the temperature profile is again found by separation of variables with the eigenvalue problem the same as before except that the boundary condition at $\xi = 1$, Eq. 19b, is replaced by

$$\frac{dX(1)}{d\xi} = 0 \tag{19c}$$

Note that the eigenvalue problems for all three wall conditions we are considering can be treated together inasmuch as the isothermal and insulated wall problems simply involve special choices of N. In all cases the c_i are found from Eq. 20.

Solution to the Eigenvalue Problem

The key to obtaining the temperature profiles is the solution to the eigenvalue problem in Eqs. 18 and 19. For arbitrary velocity fields $\phi(\xi)$, it is difficult to find an exact solution to these equations. Here we obtain approximate, asymptotically valid solutions to this problem by using the WKB-J method (Bender and Orszag, 1978). Strictly speaking, the method can be expected to give results that are accurate only for the large eigenvalues; however, it will be seen that good approximations are obtained even for the lowest eigenvalues.

We postulate a solution to Eq. 18 of the form

$$X(\xi) \sim \exp\left[\frac{1}{\delta}\sum_{n=0}^{\infty}\delta^n S_n(\xi)\right] \qquad (\delta \to 0) \tag{26}$$

where δ is a small parameter that depends on a. Inserting Eq. 26 into Eq. 18 yields

$$\frac{1}{\delta^2}[(S_0')^2 + 2\delta S_0'S_1' + \ldots] + \frac{1}{\delta}[S_0'' + \delta S_1'' + \ldots] + a\phi = 0 \quad (27)$$

in which $'$ denotes a derivative with respect to ξ. The two dominant terms in this series must be $(S_o')^2/\delta^2$ and $a\phi$. For these to be the same order of magnitude we require

$$\delta = a^{-1/2} \quad (28)$$

Substituting Eq. 28 into Eq. 27 and equating equal orders in a gives differential equations for the $S_n(\xi)$. The first two of these yield

$$S_0 = \pm i \int^{\xi} \sqrt{\phi(\xi')}d\xi' \quad (29)$$

$$S_1 = \ln \phi^{-1/4} + A_1 \quad (30)$$

We assume that the eigenvalues are large enough so that the series can be approximated by the leading two terms.

When the symmetry condition, Eq. 19a, is applied, the WKB-J approximation to the eigenfunction becomes

$$X(\xi) \sim A_2\phi^{-1/4}(\xi) \cos\left[\sqrt{a}\int_0^{\xi}\sqrt{\phi}d\xi'\right] \quad (31)$$

Note that Eq. 31 applies equally to the isothermal wall, insulated wall, and arbitrary Biot modulus problems. It is not possible to evaluate the eigenvalues directly by applying the wall boundary condition to Eq. 31, because the eigenfunction in Eq. 31 is singular at $\xi = 1$ by virtue of the no-slip condition on velocity at that point. To remedy this situation, we introduce a boundary layer solution near the wall by expanding the velocity field in a Taylor series about $\xi = 1$, and substitute this result to order $(1 - \xi)$ into Eq. 18:

$$X'' + a\dot{\gamma}_w(1 - \xi)X = 0 \quad (32)$$

where $\dot{\gamma}_w$ is the dimensionless wall shear rate. By using the boundary condition in Eq. 19b for arbitrary Biot modulus, the solution to Eq. 32 is found in terms of Airy functions to be

$$X(\xi) \sim A_3\left\{Ai[-(\dot{\gamma}_w a)^{1/3}(1 - \xi)] + \frac{\left[3^{5/6}\Gamma\left(\frac{2}{3}\right) - 3^{1/2}(\dot{\gamma}_w a)^{-1/3}N\Gamma\left(\frac{1}{3}\right)\right]}{3\left[3^{1/3}\Gamma\left(\frac{2}{3}\right) + (\dot{\gamma}_w a)^{-1/3}N\Gamma\left(\frac{1}{3}\right)\right]} \times Bi[-(\dot{\gamma}_w a)^{1/3}(1 - \xi)]\right\} \quad (33)$$

The corresponding eigenfunction for the insulated wall is readily obained by setting $N = 0$ in Eq. 33.

To determine the eigenvalue a, we look for a matching region where the eigenfunctions in Eqs. 31 and 33 exhibit similar characteristics. In the interval where the solutions overlap, Eq. 31 behaves as $(\xi \to 0)$

$$X(\xi) \sim A_2[\dot{\gamma}_w(1 - \xi)]^{1/4} \cos\left\{\frac{2}{3}[(\dot{\gamma}_w a)^{1/3}(1 - \xi)]^{3/2} - \sqrt{a}\int_0^1\sqrt{\phi}d\xi\right\} \quad (34)$$

and Eq. 33 behaves as $((1 - \xi)(\dot{\gamma}_w a)^{1/3} \to \infty)$

$$X(\xi) \sim \frac{-A_3}{\sqrt{\pi}} \frac{[(\dot{\gamma}_w a)^{1/3}(1 - \xi)]^{-1/4}}{\sin\alpha} \cos\left\{\frac{2}{3}[(\dot{\gamma}_w a)^{1/3}(1 - \xi)]^{3/2} + \frac{\pi}{4} + \alpha\right\} \quad (35)$$

where

$$\alpha = \tan^{-1}\left\{\frac{-3\left[3^{1/3}\Gamma\left(\frac{2}{3}\right) + (\dot{\gamma}_w a)^{-1/3}N\Gamma\left(\frac{1}{3}\right)\right]}{[3^{5/6}\Gamma\left(\frac{2}{3}\right) - 3^{1/2}(\dot{\gamma}_w a)^{-1/3}N\Gamma\left(\frac{1}{3}\right)]}\right\} \quad (36)$$

In order for the two functions in Eqs. 34 and 35 to match, we require that they be in phase with one another. Hence the eigenvalues are given by

$$a_j = \left[\frac{\left(j - \frac{1}{4}\right)\pi - \alpha}{\int_0^1\sqrt{\phi}d\xi}\right]^2 \quad (37)$$

where $j = 1,2,\ldots$ and $\pi/3 \leq \alpha \leq 2\pi/3$.

For the adiabatic and isothermal problems, the eigenvalues are obtained from Eq. 37 by letting $N = 0$ and ∞, respectively. For $N = 0$, the correct value for a_1 is zero, as it is easy to verify directly from Eq. 18 that when $a = 0$ any constant will satisfy Eqs. 18, 19a and 19c. The WKB-J method canot be expected to give this zero value since the assumption that $\delta = a^{-1/2}$ is small is clearly violated for $a = 0$. If more accurate representations to the lowest eigenvalues are needed than are given by Eq. 37, the method of Stodola and Vianello can be used (Hildebrand, 1976). More will be said about this method later.

We thus have the eigenfunction in two parts: far away from the wall, the X_i are given by Eq. 31; and near the wall, the X_i are given by Eq. 33. The next step is to join these two expressions into a uniform solution that is valid from the center to the wall of the slit. The standard procedure is to sum the core solution with the wall solution and subtract off the matching solution given by Eq. 34. Alternatively Langer (Nayfeh, 1973) suggested a more general technique for deriving the uniformly valid solution to Eq. 18. The idea behind this method consists of introducing a new dependent variable that eliminates the turning point problem, namely the location where the velocity goes to zero. The details of this method can be found in the text by Nayfeh (1973). For the present problem the uniform solution following Langer's approach is given by:

$$X_j(\xi) \sim \phi^{-1/4}\left(\sqrt{a_j}\int_{\xi}^1\sqrt{\phi}d\xi'\right)^{1/2} \times \left\{3^{1/3}\Gamma\left(\frac{2}{3}\right)J_{-1/3}\left(\sqrt{a_j}\int_{\xi}^1\sqrt{\phi}d\xi'\right) + (\dot{\gamma}_w a)^{-1/3}N\Gamma\left(\frac{1}{3}\right)J_{1/3}\left(\sqrt{a_j}\int_{\xi}^1\sqrt{\phi}d\xi'\right)\right\} \quad (38)$$

The uniformly valid eigenfunction in Eq. 38 can easily be verified to be identical to the solutions in Eqs. 31 and 33 in their respective regions of validity. The uniformly valid eigenfunction for the adiabatic wall condition is obtained by allowing $N = 0$. Finally the eigenfunction in Eq. 38 is determined only to within an arbitrary constant multiplier, since the governing equations for X_i are homogeneous.

Illustrative Examples

For the purpose of illustrating the steps required to arrive at the temperature profiles we use the power-law model. The velocity field for a power-law fluid in slit flow is given in Eq. 5, and the shear rate dependence of the viscosity is provided by Eq. 8. In order to compare our results with the finite difference solution of Ybarra and Eckert (1980), we consider the cases of $N = 0$ which corresponds to an insulated wall and $N \to \infty$ which corresponds to an isothermal wall. The fully developed temperature profiles and the eigenvalues are given respectively by

Adiabatic ($N = 0$):

$$\theta_1(\xi) = (s + 1)^{1/s}\left[\frac{\xi^2}{2} - \frac{\xi^{s+3}}{(s+3)}\right] \quad (39)$$

TABLE 1. COMPARISON OF APPROXIMATE AND EXACT EIGENVALUES FOR SLIT FLOW WITH INSULATED WALL ($N = 0$)

j \ a_j	$n = 1.0$ WKB-J	$n = 1.0$ Num.*	% diff.	$n = 0.5$ WKB-J	$n = 0.5$ Num.*	% diff.
1	0.1111	0.0000	—	0.0968	0.0000	—
2	18.778	18.388	2.120	16.365	15.837	3.334
3	69.444	68.951	0.716	60.521	59.856	1.111
4	152.11	151.63	0.317	132.566	131.84	0.550
5	266.78	266.31	0.176	232.50	231.77	0.314
6	413.44	413.03	0.100	360.32	359.62	0.194

* Ybarra and Eckert (1980).

$$a_j = \left[2\sqrt{\pi} \frac{\Gamma\left(\frac{3}{2} + \frac{1}{1+s}\right)}{\Gamma\left(1 + \frac{1}{1+s}\right)} \left(j - \frac{11}{12}\right) \right]^2 \qquad j = 1,2,3 \ldots \quad (40)$$

Isothermal wall ($N = \infty$):

$$\theta_1(\xi) = \frac{(s+1)^{1/s+1}}{(s+2)(s+3)} [1 - \xi^{s+3}] \quad (41)$$

$$a_j = \left[2\sqrt{\pi} \frac{\Gamma\left(\frac{3}{2} + \frac{1}{1+s}\right)}{\Gamma\left(1 + \frac{1}{1+s}\right)} \left(j - \frac{7}{12}\right) \right]^2 \qquad j = 1,2,3 \ldots \quad (42)$$

The eigenvalues for a power-law fluid in slit flow, with $s = 1.0$ and $s = 2.0$, are tabulated inTable 1 for an insulated wall and in Table 2 for an isothermal wall. The approximate results are compared to the numerical results obtained by Ybarra and Eckert (1980). In each case the percentage difference between the approximate and the numerical results is less than 1% except for the lowest eigenvalues where a difference of 8.53% is observed for the isothermal wall in Table 2. These relative differences are expected because we have assumed that the eigenvalues are sufficiently large so that the exponential series for the eigenfunction (Eq. 26) can be truncated after two terms. For this problem we note that the error introduced from a two-term approximation is not very serious, particularly for eigenvalues beyond the lowest ones. In principle we can compute the lowest eigenvalues to arbitrary accuracy by carrying more terms in the exponential series, or by resorting to another approximation technique such as the method of Stodola and Vianello (Hildebrand, 1976). Because it is easy to guess the correct lowest eigenvalue for the adiabatic calculations, we replace the WKB-J approximation by $a_1 = 0$ for the temperature calculations below.

Once the eigenvalues are known, the eigenfunctions are evaluated from Eq. 38, and the expansion coefficients are determined from Eq. 20. The temperature field is then calculated from Eq. 14 or Eq. 21 depending on the wall condition. The local temperature profiles determined in this way show negligible difference from those of Ybarra and Eckert for each case considered as would be expected from the eigenvalue agreement.

To facilitate comparison between the power-law results and those for a Newtonian fluid, we have plotted the temperature profiles in a dimensionless form based on the average fluid velocity $\langle v \rangle$ rather than the maximum velocity. Thus, Figures 2–6 present $\bar{\theta}$ as a function of ξ for various axial locations $\bar{\zeta}$ where $\bar{\theta}$ and $\bar{\zeta}$ are defined by:

$$\bar{\theta} = \frac{(T - T_o)k}{\langle v \rangle^2 \eta_0}; \quad \bar{\zeta} = \frac{kz}{\rho \hat{C}_p \langle v \rangle B^2} \quad (43)$$

For power-law fluids we now take η_o to be the power-law viscosity evaluated at the shear rate $\dot{\gamma} = \langle v \rangle / B$, so that $\eta_o \equiv m(\langle v \rangle / B)^{n-1}$; then $\bar{\theta}$ and $\bar{\zeta}$ are related to θ and ζ by

$$\bar{\theta} = \theta \left(\frac{s+2}{s+1}\right)^{n+1} \quad (44)$$

$$\bar{\zeta} = \zeta \left(\frac{s+2}{s+1}\right) \quad (45)$$

By comparing Figures 2 and 3 for the adiabatic problem and Figures 4 and 5 for the isothermal wall problem it can be seen that for equal volume flow rates and for $m(\langle v \rangle / B)^{n-1} = \mu$, the effect of shear thinning is to lower the amount of viscous heating and the resulting temperature rise in the power-law fluid relative to the Newtonian fluid.

In order to investigate the effect of the Biot number on the temperature field we consider next Newtonian slit flow for variable N. To compute the eigenvalues for various N we use Eq. 37. Notice that since a_j appears with N in the phase angle α (Eq. 36), Eq. 37 is implicit in a_j. To obtain values for a_j we used successive approximations: We first assume a value for a_j (between the adiabatic and isothermal values), evaluate α and then calculate a_j from Eq. 37 with the right side known. The new value for a_j is used to obtain a better estimate for α, and so on. Only a few iterations are required. The results of these calculations are given in Table 3 where we list the lowest eigenvalue a_1 for a wide range of Biot number. We chose to list the lowest eigenvalue here because the WKB-J approximation to it will be worst. Also we have used the method of Stodola and Vianello with a quadratic trial function for the temperature profile to obtain a second estimate of a_1 for comparison. From comparing the Stodola and Vianello approximations to a_1 for $N = 0$ and $N = \infty$ with exact numerical results, it can be seen that the Stodola and Vianello method gives very accurate estimates for the lowest eigenvalues even after only one iteration (which is all we used). Then comparison of a_1 from the WKB-J and Stodola and Vianello methods for N between 0 and ∞ shows that the WKB-J approximation is quite good provided the exact a_1 is greater than the WKB-J approxiation for the adiabatic a_1. The temperature profile which corresponds to the $N = 1$ Biot number

TABLE 2. COMPARISON OF APPROXIMATE AND EXACT EIGENVALUES FOR SLIT FLOW WITH ISOTHERMAL WALL ($N = \infty$)

j \ a_j	$n = 1.0$ WKB-J	$n = 1.0$ Num.*	% diff.	$n = 0.5$ WKB-J	$n = 0.5$ Num.*	% diff.
1	2.7778	2.8278	1.769	2.4208	2.6466	8.530
2	32.111	32.147	0.112	27.985	28.132	0.522
3	93.444	93.473	0.031	81.437	81.566	0.158
4	186.78	186.80	0.012	162.78	162.89	0.069
5	312.11	312.12	0.003	272.07	272.11	0.015
6	469.44	469.42	0.005	409.12	409.20	0.019

* Ybarra and Eckert (1980).

TABLE 3. COMPARISON OF THE LOWEST EIGENVALUES FROM DIFFERENT METHODS FOR NEWTONIAN SLIT FLOW WITH VARIOUS BIOT MODULI

Biot Number, N \ Method	WKB-J	Stodola-Vianello	Numerical*
0	0.1111	0	0
10^{-3}	0.1128	0.00146	—
10^{-2}	0.1274	0.0146	—
10^{-1}	0.2564	0.1465	—
1	1.0509	1.1384	—
10	2.3711	2.4589	—
10^{2}	2.7311	2.7881	—
10^{3}	2.7730	2.8242	—
∞	2.7778	2.8283	2.8278

* Ybarra and Eckert (1980).

is shown in Figure 6. As expected, the shapes of the developing profiles are intermediate to the adiabatic and isothermal results and there are relatively steep temperature gradients at the wall.

TUBE PROBLEM

In this problem we consider the local temperature change of a non-Newtonian fluid flowing in a tube as depicted in Figure 1. The tube radius is R and once again we assume the fluid reaches $z = 0$ at uniform temperature T_o and with a fully developed velocity profile. The assumptions used to simplify the governing equation for the dimensionless temperature field are identical to those employed in the slit flow problem. The energy equation in cylindrical coordinates is thus written as:

$$\phi \frac{\partial \theta}{\partial \zeta} = \frac{1}{\xi} \frac{\partial}{\partial \xi} \left(\xi \frac{\partial \theta}{\partial \xi} \right) + \eta_r \left(\frac{d\phi}{d\xi} \right)^2 \tag{46}$$

with the following boundary conditions:

$$\text{at } \zeta = 0, \theta = 0 \tag{47}$$

$$\text{at } \xi = 0, \frac{\partial \theta}{\partial \xi} = 0 \tag{48}$$

$$\text{at } \xi = 1, \frac{\partial \theta}{\partial \xi} = -N\theta, \text{ "arbitrary" heat transfer} \tag{49a}$$

$$\frac{\partial \theta}{\partial \xi} = 0, \text{ adiabatic} \tag{49b}$$

in which $\xi = r/R$ is now a dimensionless radial coordinate.

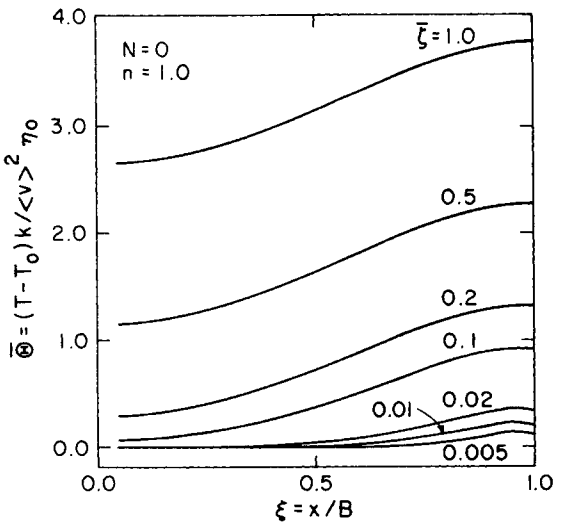

Figure 2. Dimensionless temperature as a function of position for adiabatic, Newtonian slit flow.

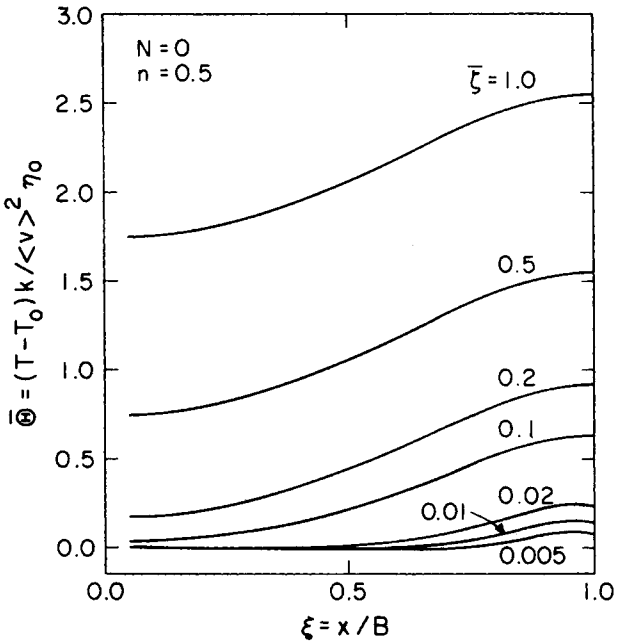

Figure 3. Same as Figure 2 but for a power-law fluid with power-law index $n = 0.5$.

We again postulate solutions to the temperature profile which consist of separate developing and fully developed parts. These are Eqs. 14 and 21 for the non-zero Biot modulus and insulated wall, respectively. The fully developed parts to the solution are now

Arbitrary wall heat transfer:

$$\theta_1(\xi) = \frac{1}{N} \int_0^1 \xi' \eta_r(\xi') \left(\frac{d\phi}{d\xi'} \right)^2 d\xi' + \int_\xi^1 \frac{1}{\xi'} \int_0^{\xi'} \xi'' \eta_r(\xi'') \left(\frac{d\phi}{d\xi''} \right)^2 d\xi'' d\xi' \tag{50}$$

Insulated wall:

$$\theta_1(\xi) = \int_0^\xi \frac{1}{\xi'} \int_0^{\xi'} \xi'' \left[\phi(\xi'') D_0 - \eta(\xi'') \left(\frac{d\phi}{d\xi''} \right)^2 \right] d\xi'' d\xi' \tag{51}$$

where,

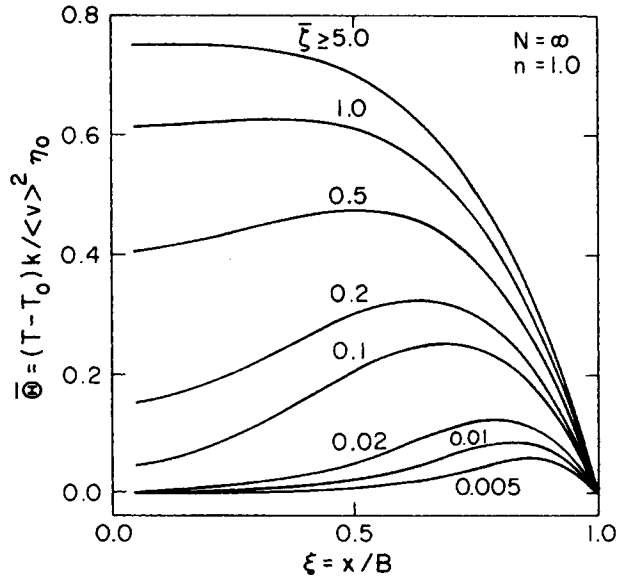

Figure 4. Dimensionless temperature as a function of position for Newtonian slit flow. The wall is isothermal.

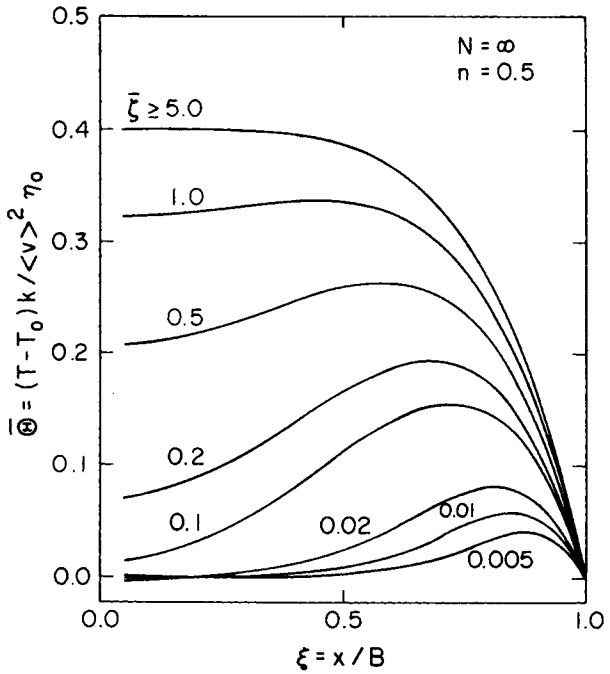

Figure 5. Same as Figure 4 except for a power-law fluid with power-law index $n = 0.5$.

$$D_0 = \frac{\int_0^1 \xi\eta_r(\xi)\left(\frac{d\phi}{d\xi}\right)^2 d\xi}{\int_0^1 \xi\phi(\xi)d\xi} \tag{52}$$

The eigenfunctions for the transient profile satisfy the following differential equation:

$$\frac{d}{d\xi}\left(\xi\frac{dX}{d\xi}\right) + a\xi\phi X = 0 \tag{53}$$

with

$$\xi = 0, \frac{dX}{d\xi} = 0 \tag{54a}$$

$$\xi = 1, \frac{dX}{d\xi} = -NX \tag{54b}$$

The limiting case of $N = 0$ corresponds to the insulated wall condition.

The WKB-J method is employed to determine the eigenfunctions and eigenvalues in the same manner as described for the slit flow problem. In developing the boundary layer solution near the wall we assume that the curvature of the channel is negligible. Therefore, the eigenfunction near the wall is identical to the solution obtained in the slit flow problem, namely Eq. 23. Away from the wall the WKB-J method gives the following sinusoidal approximation to the eigenfunctions

$$X(\xi) \sim A_2\left(\frac{2}{\pi\xi\sqrt{a\phi}}\right)^{1/2}\cos\left(\sqrt{a}\int_0^\xi\sqrt{\phi}d\xi' - \frac{\pi}{4}\right) \tag{55}$$

However, Eq. 55 breaks down at the center of the channel because ξ appears in the denominator. To remedy this situation we introduce another boundary layer solution in this interval. A reasonable approximation is to expand the dimensionless velocity in a Taylor series about the centerline and retain the leading term; hence $\phi \sim 1$. This assumption reduces the differential equation to a soluble form in terms of Bessel functions of order 0. Applying the symmetry condition at the center of the tube gives

$$X(\xi) \sim A_1 J_0(\sqrt{a}\xi) \qquad (\xi \to 0) \tag{56}$$

To determine the eigenvalues we search for a matching region where the eigenfunctions in Eqs. 33 and 55 overlap. As in the argument presented in the previous section, these two functions must be in phase in matching interval; thus the eigenvalues are given by

$$a_j = \left[\frac{j\pi - \alpha,}{\int_0^1\sqrt{\phi}d\xi}\right] \tag{57}$$

where $j = 1,2,\ldots$ and $\pi/3 < \alpha < 2\pi/3$. The angle α is given in Eq. 36.

In principle the eigenfunction in Eqs. 31, 53, and 54 can be used to evalute the temperature profile; however, it is practically difficult to do this since it is a hard problem to determine the precise bounds over which each of these approximations to the eigenfunction should be used. A more straightforward method for obtaining temperature is to use the uniformly valid approximation to the eigenfunction obtained by Langer's method. Langer's method applied here gives

$$X_j(\xi) \sim (a_j\xi^2\phi)^{-1/4}\left(\sqrt{a_j}\int_\xi^1\sqrt{\phi}d\xi'\right)^{1/2} \times\left\{3^{1/3}\Gamma\left(\frac{2}{3}\right)J_{-1/3}\left(\sqrt{a_j}\int_\xi^1\sqrt{\phi}d\xi'\right) + (\dot{\gamma}_w a)^{-1/3}N\Gamma\left(\frac{1}{3}\right)J_{1/3}\left(\sqrt{a_j}\int_\xi^1\sqrt{\phi}d\xi'\right)\right\} \tag{58}$$

Temperature profiles can now be obtained from the eigenvalues (Eq. 57) and the eigenfunctions (Eq. 58) for any non-Newtonian viscosity function by using the same procedure outlined in the section, "Slit Problem." The only change required is that the expansion coefficients be computed from

$$c_i = \frac{\int_0^1\theta_1(\xi)X_i(\xi)\xi d\xi}{\int_0^1\phi(\xi)X_i^2(\xi)\xi d\xi} \tag{59}$$

instead of Eq. 20.

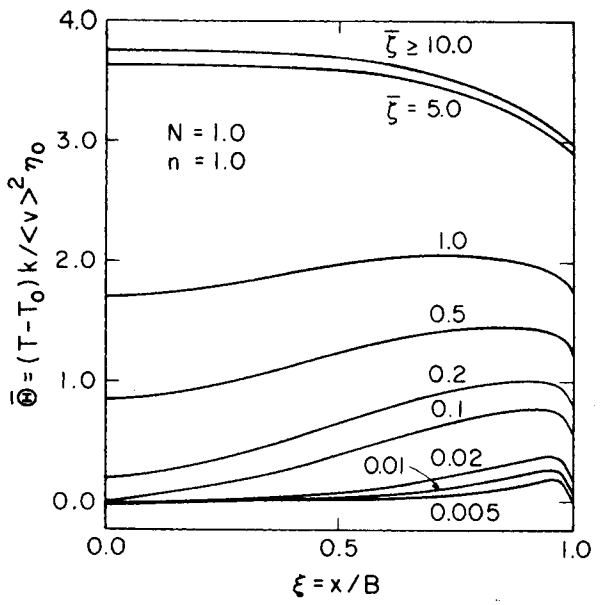

Figure 6. Dimensionless temperature as a function of position for Newtonian slit flow with Biot modulus $N = 1.0$.

CONCLUSIONS

The main results of this paper are the uniformly valid eigenfunction expressions in Eqs. 38 and 58 for the slit and tube flow

problems, respectively. These have not been previously reported and are necessary in order to compute the temperature profiles accurately.

For both the slit flow problem and the tube flow problem, the lowest eigenvalues—which will be the least accurate—obtained by the WKB-J method are in good agreement (~10% error in the worst case) with numerical results. The higher eigenvalues are practically indistinguishable from the numerical values.

Although we have restricted the development to low Nahme-Griffith number problems (small temperature changes or temperature insensitive viscosity) the results are more generally useful, we feel. In particular, in numerical simulations of high Nahme-Griffith number problems such as that by Winter (1977), formulas developed here can aid in reducing the iterations required to obtain a solution. This reduction could be particularly valuable when such programs are incorporated as part of a large polymer processing simulation.

ACKNOWLEDGMENTS

The authors are grateful to the MIT-Industry Polymer Processing Program for financial support of this work.

NOTATION

a_i = eigenvalues
A_1, A_2, A_3 = constants of integration
$Ai(x), Bi(x)$ = airy functions
B = half thickness or radius of the channel
c_i = expansion coefficients
$\hat{C}_p$ = heat capacity, J/kg K
D_o = constant defined in Eqs. 25 and 52
h = heat transfer coefficient, g/(s^3 K)
J_γ = Bessel function of the first kind of order γ
k = thermal conductivity, W/m K
m = consistency index in power law model, Eq. 4
n = power law exponent, Eq. 4
N = hB/k, Biot number
s = reciprocal of the power law index
T = temperature, K
T_o = reference temperature, K
v = velocity, m/s
$\langle v \rangle$ = average velocity, m/s
X_i = eigenfunctions

Greek Letters

α = angle defined in Eq. 36
$\Gamma(x)$ = gamma function
$\dot{\gamma}_w$ = dimensionless wall shear rate
ζ = $\dfrac{kz}{\rho \hat{C}_p V_{\max} B^2}$, dimensionless axial coordinate
$\bar{\zeta}$ = $\dfrac{kz}{\rho \hat{C}_p \langle v \rangle B^2}$, dimensionless axial coordinate (Eq. 45)
η = non-Newtonian viscosity, Pa • s
η_o = zero shear rate viscosity, Pa • s
η_r = dimensionless function representing the dependence of the viscosity on the rate of deformation
θ = $\dfrac{(T - T_o)k}{V_{\max}^2 \eta_o}$, dimensionless temperature
$\bar{\theta}$ = $\dfrac{(T - T_o)k}{\langle v \rangle^2 \eta_o}$, dimensionless temperature (Eq. 44)
ξ = $\begin{cases} x/B, \text{ dimensionless transverse coordinate} \\ r/B, \text{ dimensionless radial coordinate} \end{cases}$
ρ = density, g/cm^3
ϕ = $\dfrac{v}{V_{\max}}$, dimensionless velocity

LITERATURE CITED

Acrivos, A., "The Extended Graetz Problem at Low Peclet Numbers," *Appl. Sci. Res.*, **36**, 1, 35 (1980).

Bender, C. M. and S. A. Orszag, *Advanced Mathematical Methods for Scientists and Engineers*, McGraw-Hill Book Co., 484 (1978).

Gerrard, J. E., R. E. Steidler, and J. K. Appeldoorn, "Viscous Heating in Capillaries. The Adiabatic Case," *I&EC Fund.*, **4**, 332 (1965).

Gerrard, J. E., F. E. Steidler, and J. K. Appeldorn, "Viscous Heating in Capillaries. The Isothermal-Wall Case," *I&EC Fund.*, **5**, 260 (1966).

Hildebrand, F. B., *Advanced Calculus for Applications*, Prentice-Hall Inc., 197 (1976).

Jakob, M., *Heat Transfer*, John Wiley & Sons, Inc., 1 (1949).

Nayfeh, A., *Perturbation Methods*, John Wiley & Sons, 335 (1973).

Ockendon, H., "Channel Flow with Temperature-dependent Viscosity and Internal Viscous Dissipation," *J. Fluid Mech.*, **93**, 4, 737 (1979).

Papoutsakis, E., D. Ramkrishna and H. C. Lim, "The Extended Graetz Problem with Dirichlet Wall Boundary Conditions," *Appl. Sci. Res.*, **36**, 1, 13 (1980).

Pearson, J. R. A., "Polymer Flows Dominated by High Heat Generation and Low Heat Transfer," *Polym. Eng. Sci.*, **18**, 1, 222 (1978).

Sellars, J. R., M. Tribus, and J. S. Klein, "Heat Transfer to Laminar Flow in a Round Tube or Flat Conduit—The Graetz Problem Extended," *Trans. ASME*, **78**, 441 (1956).

Winter, H. H., "Viscous Dissipation in Shear Flow of Molten Polymers," *Adv. Heat Transf.*, **13**, 205 (1977).

Ybarra, R. M. and R. E. Eckert, "Viscous Heat Generation in Slit Flow," *AIChE J.*, **26**, 5, 751 (1980).

Ziegenhagen, A. J., "Approximate Eigenvalues for Heat Transfer to Laminar or Turbulent Flow in an Annulus," *Int. J. Heat Mass Transf.*, 8, 499 (1965).

Manuscript received July 31, 1980; revision received May 18, and accepted June 22, 1981